CONF-8809218--2
Talk given at Mainz, Germany
September 1988

A Study of $K^+ \to \pi^+\nu\bar{\nu}$

BNL--42146
DE89 007074

M.S. Atiya, I-H. Chiang, J.S. Frank, J.S. Haggerty, M. Ito,
T.F. Kycia, K.K. Li, L.S. Littenberg, A.J. Stevens, R.C. Strand

Brookhaven National Laboratory, Upton, NY 11973

W.C. Louis

Los Alamos National Laboratory, Los Alamos, NM 87545

D.S. Akerib, D.R. Marlow, P.D. Meyers,
M.A. Selen, F.C. Shoemaker, A.J.S. Smith

Physics Department, Princeton University, Princeton, NJ 08544

G. Azuelos, E.W. Blackmore, D.A. Bryman, L. Felawka,
P. Kitching, Y. Kuno, J. Macdonald, T. Numao,
P. Padley, J-M. Poutissou, R. Poutissou, J. Roy

TRIUMF, Vancouver, BC V6T 2A3 CANADA

(Presented by K.K. Li)

Received by OSTI
FEB 21 1989

ABSTRACT

A description of the detector and of preliminary results of work in progress in its performance is presented here for an experiment to study the decay of $K^+ \to \pi^+\nu\bar{\nu}$.

Experiment E787 at the Brookhaven AGS was designed to study the rare decay of the positively charged kaon into $\pi^+\nu\bar{\nu}$. The present limit on the BR of this decay, established by previous experiments[1] with the latest by Asano et al.,[2] in 1981, is 1.4×10^{-7}. This strangeness changing neutral current process is strongly suppressed[3]. Results of higher order calculations[4] in the Standard Model, depending upon the top quark mass and the number of ν generations, are $O(10^{-10})$. There is a span of about three orders of magnitude between the present limit and the predictions. A result substantially higher than the predictions, say several times 10^{-9}, would indicate new physics. Possibilities for this could be more quark generations, or indications of the existence of new neutral, light and weakly interacting particles. A result in agreement with the Standard Model prediction would provide a theoretically clean check of the higher order weak interaction picture, and provide constraints for further attempts beyond the Standard Model.

As this decay is kinematically underconstrained and the π^+ spectrum overlaps with other more dominant decay modes as shown in Fig. 1, it is

MASTER

DISTRIBUTION OF THIS DOCUMENT IS UNLIMITED

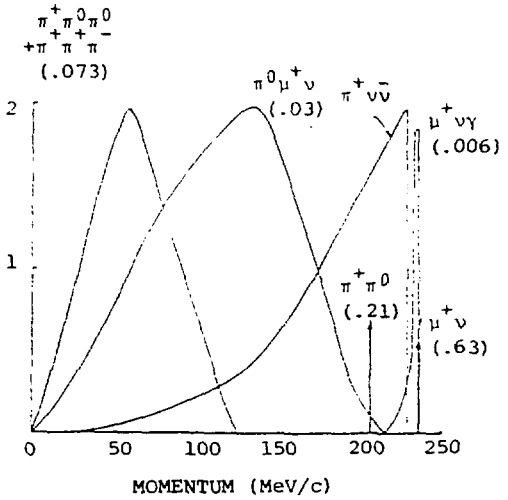

FIGURE 1
Momentum distribution of π^+ for various K^+ decay modes

necessary to positively identify the π^+ by all possible means and to reject backgrounds to the highest degree possible. To do this, we chose to study with K^+ decays at rest. To avoid the $K_{\pi 2}$ background due to π^+ interactions, we chose to concentrate on the kinematic region above the $K_{\pi 2}$ peak, which yields ~ 20% of the spectrum. The π^+ is measured independently in energy, momentum and range, and identified through its characteristic decay chain of $\pi^+ \rightarrow \mu^+ \rightarrow e^+$ with a 4 MeV μ^+. Full 4π coverage of γ detection with high efficiency even at low energy is needed. Higher kaon flux, larger solid angle and better background suppression are needed to achieve a factor of about 600 in sensitivity improvement over the previous measurement. A detector was built for this study to probe the BR down to 2×10^{-10}. A schematic layout is shown in Fig. 2 with dimensions shown in Table 1. It is axially symmetric.

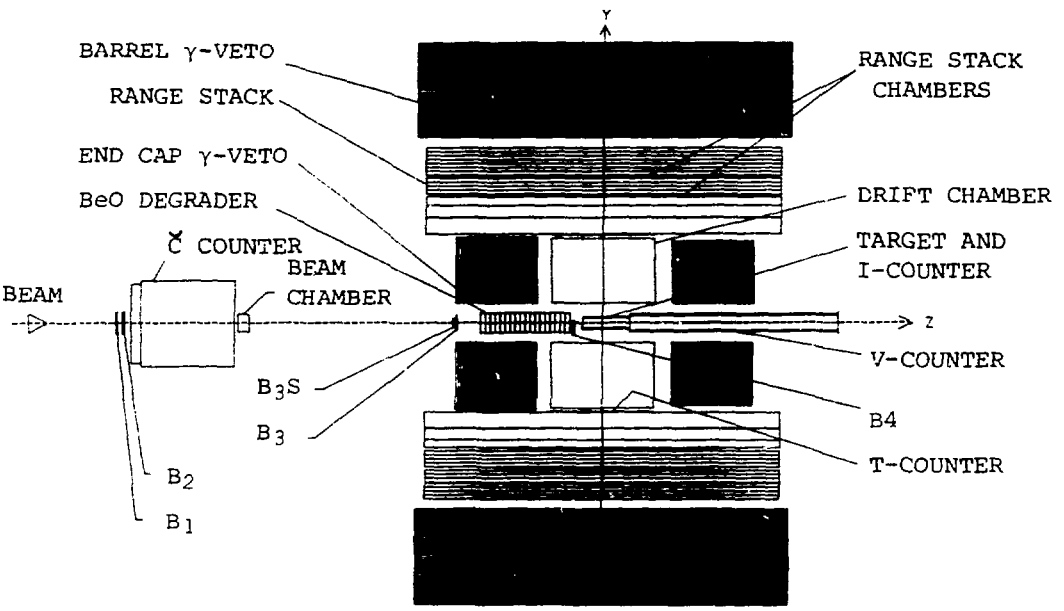

FIGURE 2
Schematic layout of the detector

The 775 MeV/c mass separated beam LESB1 from the AGS passes through a series of beam counters and chambers with the K^+ identified by a

differential Cerenkov counter. The K^+, after passing through a BeO degrader, stops inside a scintillation fiber target. The π^+ from the decay is tracked through the central drift chamber where its momentum is measured, comes to stop inside a stack of 15 layers of scintillation counters (Range Stack), and decays through the chain $\pi^+ \rightarrow \mu^+ \rightarrow e^+$. Two layers of chambers are interspersed in the Range Stack to refine the range measurements. Surrounding the Range Stack radially and on both ends of the drift chamber is a system of lead-scintillator γ detector (Barrel Veto and End Caps). The complete detector is housed inside a 10KG magnet with ~ 2 ft. of steel all around. The detector is highly segmented in the azimuth, with the Range Stack and the γ detector systems having 24 identical azimuthal-sectors. To reduce cracks in γ detection, the Barrel Veto sector boundaries are oriented away from the target. The light from the scintillation counter is piped through the 2 ft. of steel to PMT's mounted outside. All Range Stack and Barrel Veto counters are read from both ends. All counter channels are instrumented with ADC's and TDC's.

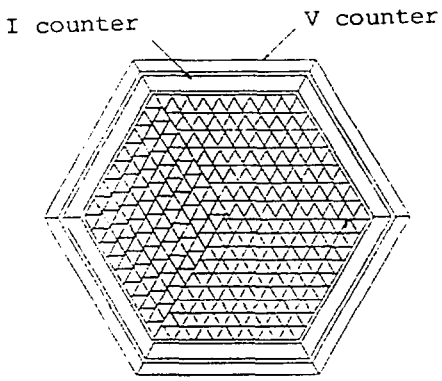

FIGURE 3
End view of fiber target. I & V are coincident & anti-coincident counters, triangles are 6-fiber clusters

There are two perhaps somewhat unconventional aspects of the detector. One is the finely segmented scintillation fiber target that locates the K^+ decay vertex. Figure 3 shows a schematic end view of the target . The other is a system of 500 MHz transient digitizers (TD) with fast read out developed for this experiment. All Range Stack counters in the $\pi^+\nu\bar{\nu}$ range region are instrumented with this digitizer which provides essentially a scope trace for the $\pi^+ \rightarrow \mu^+ \rightarrow e^+$ decay with a time window of 10 μsec, 5 μsec before and 5 μsec after the prompt. Thus there is a space-time map for each event.

The detector completed its first run last May. It was devoted mostly to calibrations and establishing triggers. The trigger is arranged in three levels of increasing complexity. The highest level is by software making use of the energy and transient digitizer data. Data are read from both CAMAC and FASTBUS crates. A system of special processors (SSP from SLAC) are used in the FASTBUS crates to store data during beam spill, and to perform final trigger decisions. A μVAX2 computer is used to read out data

between spills. The equivalent of about one week of data taking was made triggering on $\pi^+\nu\bar{\nu}$, $\pi^+\mu^+\mu^-$ and $\pi^+\gamma\gamma$ modes at an intensity of ~ 150K K^+ stops/spill and π/K ratio ≈ 2.5. A total of ~ 10^{10} stopped K^+ were accumulated. Data from special triggers like $K_{\pi 2}$, $K_{\mu 2}$ and π^+ scattering were also taken for calibration and monitoring.

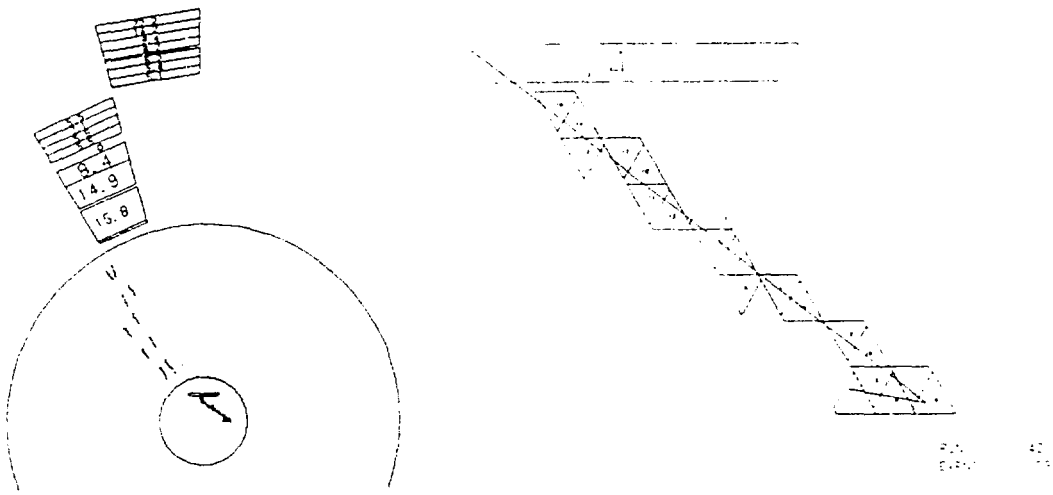

FIGURE 4
A $K_{\mu 2}$ decay candidate display with details in target. ADC and TDC information is shown respectively on the Range Stack counters and on the target

The tracks of the K^+ and the decay particle in the target are identified by timing and energy deposition. The average measured energy per cluster is ~ 25 MeV for K^+ and ~ 1 MeV for π^+. The radial spatial resolution on the decay vertex location is ~ 2 mm. An end-on view of a $K_{\mu 2}$ candidate is shown in Fig. 4 where the hit counters in the target and the Range Stack are displayed. The K^+ and the μ^+ portions of the clusters in the target are separated by ~ 10 nsec. To avoid prompts, a 2 nsec delay was required in the triggers. Figure 5 shows the K^+ decay time distribution from a sample of $K_{\mu 2}$ triggers, from which a time resolution of ~ 1 nsec is deduced.

The transient digitizer data were used at the trigger level to reject μ's by cutting on the extra area of the pulse from the stopping particle. A muon rejection of ~ 7 was achieved with ~ 70% pion efficiency. A more detailed analysis of pulse shape fitting is used off-line. Figure 6 shows a typical $\pi^+ \to \mu^+ \to e^+$ event. The μ^+ pulse is extracted by a best fit to the data with a two pulse hypothesis. The difference of the $\pi^+ - \mu^+$ time separation as measured at the two ends of the same counter is shown in Fig. 7. The μ^+ energy distribution is shown in Fig. 8. Accidentals can be

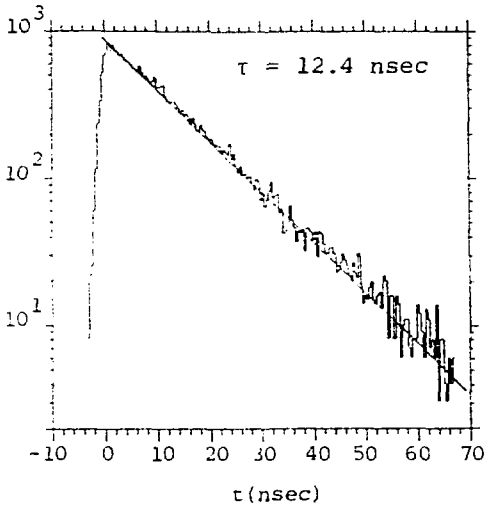

FIGURE 5
K^+ decay time distribution in target

further rejected by cuts on these parameters, and by the fact that the e^+ is energetic enough to penetrate through more than one counter. The π^+ decay time distribution is shown in Fig. 9. Figure 10 shows the μ^+ decay time distribution. An overall efficiency of ~ 70% for the e^+ finding is due mainly to the time window used.

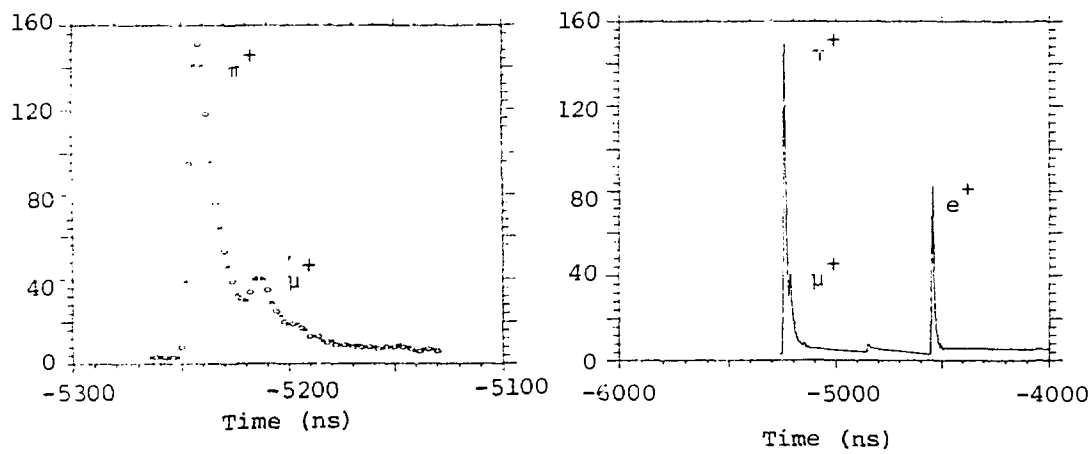

FIGURE 6
A π^+ decay as recorded by TD. Data points are separated by 2 nsec

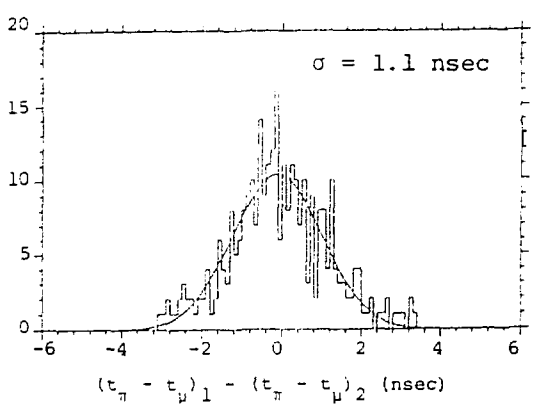

FIGURE 7
End-end difference of π^+ decay time

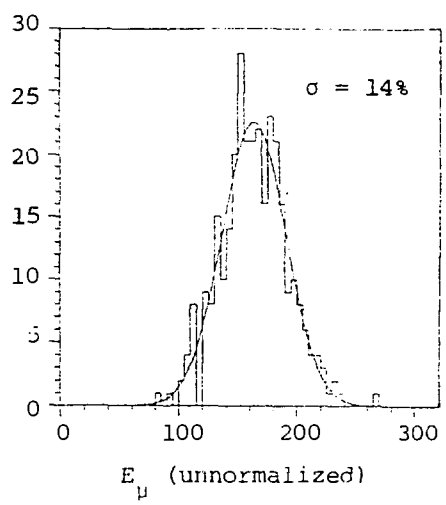

FIGURE 8
Distribution of μ^+ energy

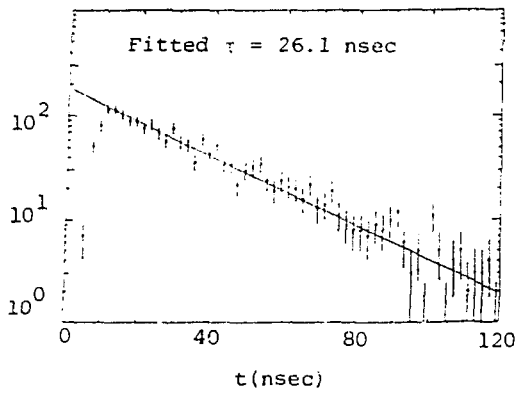

FIGURE 9
π^+ decay time distribution

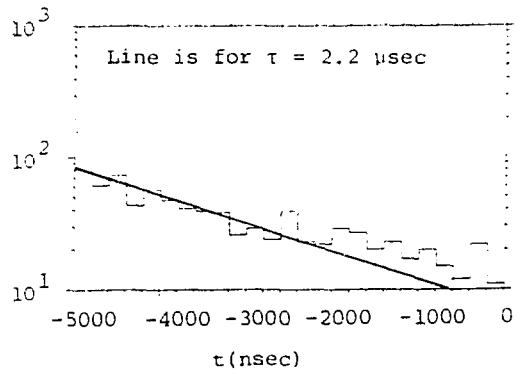

FIGURE 10
μ^+ decay time distribution

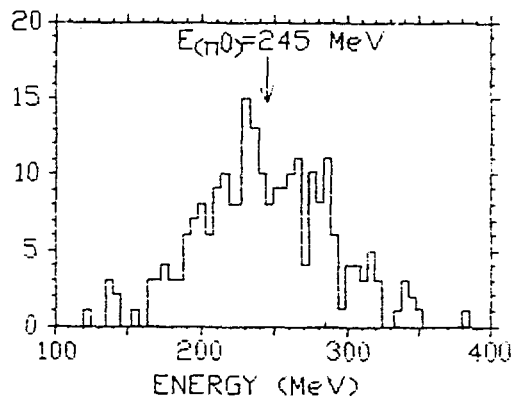

FIGURE 11
Total neutral energy in $\bar{\gamma}$ system for $K_{\pi 2}$ decays

The γ detection system was not used in the trigger for $K_{\pi 2}$. The total in-time neutral energy as seen by the system from a selected $K_{\pi 2}$ sample is shown in Fig. 11. It agrees well with the total π^0 energy expected from $K_{\pi 2}$ decays. The total π^0 detection inefficiency is obtained by using the full $\pi^+\nu\bar{\nu}$ data sample. Preliminary study of the number of events under the $K_{\pi 2}$ peak after cuts yields a π^0 rejection efficiency of $\sim 5 \times 10^{-6}$, consistent with that in the proposal. Improvement is likely with further advances on event selection.

Drift chamber resolution was studied using cosmic rays, $K_{\mu 2}$ and $K_{\pi 2}$ events. The local spatial resolution near the wire is about 150 μm. The Z resolution is about 3mm. The total momentum resolution for a $K_{\mu 2}$ sample at 10 KG is found to be $\Delta P/P \lesssim 2.5\%$.

The measurements of energy and momentum are correlated through the energy loss in the target. Similarly, range is correlated with the energy measurement of the last Range Stack counter. For a selected sample of 1522 $K_{\pi 2}$ events, the π^+ range, energy and momentum distributions after target correction, last counter correction and a consistency cut on the three variables are shown in Fig. 12. The resolutions shown are consistent with

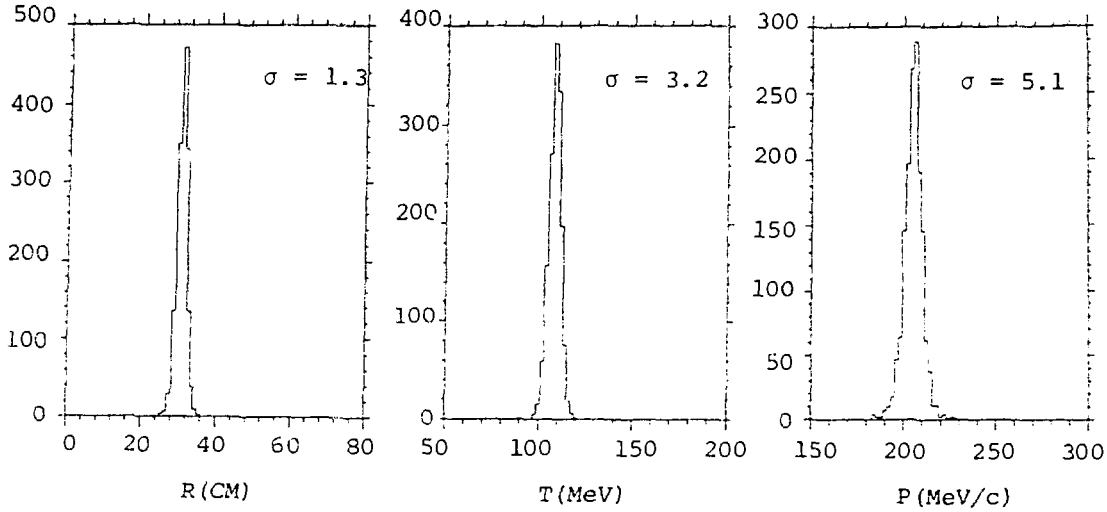

FIGURE 12
Distributions of Range, Energy and Momentum of π^+ from $K_{\pi 2}$ decays

the original estimates. Data are presently being analyzed and studies are being made on various cuts and on acceptance calculations.

REFERENCES

1) D. Ljung and D. Cline, Phys. Rev. D8, 1307 (1973); J.H. Klems, R.H. Hildebrand and R. Stiening, Phys. Rev. D4, 66 (1971); C.Y. Pang, et al., Phys. Rev. D8, 1989 (1973); G.D. Cable, et al., Phys. Rev. D8, 3807 (1973).

2) Y. Asano, et al., Phys. Lett. 107B, 159 (1981).

3) S.L. Glashow, Nucl. Phys. 22, 579 (1961); S. Weinberg, Phys. Rev. Lett. 19, 1264 (1967); A. Salam, Proc. 8th Nobel Symposium, 1968, ed. N. Svartholm; S.L. Glashow, J. Iliopoulos and L. Maiani, Phys. Rev. D2, 1285 (1970).

4) M.K. Gaillard and B.W. Lee, Phys. Rev. D10, 897 (1974); T. Inami and C.S. Lim, Prog. Theor. Phys. 65, 297 (1981); J. Ellis and J.S. Hagelin, Nucl. Phys. B217, 189 (1983); J. Ellis, J.S. Hagelin and S. Rudaz, Phys. Lett. 192B, 201 (1987); see also J.S. Hagelin, talk given at the Kaon Workshop at Brookhaven (August, 1988).

DISCUSSION:

Dydak, CERN: You did not quote a result for $BR(K^+ \to \pi^+ \nu\bar{\nu})$. Can you at least indicate whether you confirm the Asano et al., result?

Li : We are still studying our acceptances. If there is no signal in our present data sample, we estimate it will be in the order of a few times 10^{-8}.

THIS RESEARCH IS SUPPORTED IN PART BY THE U.S. DEPARTMENT OF ENERGY UNDER CONTRACT NO. DE-AC02-76CH00016.

Table 1 Dimensions of Components

Magnet	Inner Volume	2.2m(L)×2.96m(ϕ)
	Central Field	10 KG
	Fringe Field	≲ 15G at PMT's

		W(cm)	H(cm)	T(cm)
Beam Counter	B1	17.5	4	0.3
	B2	8× (2.5	4	0.3)
		4× (20	1	0.3)
	B3S	5	3.8	0.3
	B3	10	10	0.3
	B4 (dE/dX)	4× (2.5	10	0.6)
		4× (10	2.5	0.6)

Beam Chamber	3 Planes	18.3cm(W)×5cm(H)
	Gas	CF_4/isobutane (80:20)
Cerenkov Counter	Lucite radiator	2.5cm(T)×15.2cm(ϕ)
Beam Degrader	BeO	45.7cm(L)×11.4cm(ϕ)
Target	Scintillation fiber	2269×(2 mm(ϕ)×3.1 m(L)); 379 clusters; overall 10cm face-face hexagon
	I Counter	6×(23.7cm(L)×0.6cm(T))
	V Counter	6×(195.8cm(L)×0.5cm(T))
Drift Chamber	Sensitive Volume	48.9cm(L)×81.3cm(OD)×22.9cm(ID); 256 cells in 5 layers, 1536 channels; 3.5° and 3.7° stereo layers
	Gas	Ar/Ethane (50:50)
Range Stack		90cm(ID)×179cm(OD) 24 ϕ-sectors, 182cm(L)×1.9cm(T)
	Chambers	92.6cm(L)×16.9cm(W) 108.4cm(L)×19.5cm(W)
	Gas	Ar/Isobutane (75:25)
Barrel Veto		190cm(L)×191cm(ID)×293cm(OD); 75 layers of (1mm Pb+5mm scin.) 14.3 radiation length
End Caps		39.6cm(L)×21cm(ID) ×83.9cm(OD) (upstream) ×80.1cm(OD) (downstream) 66 layers of (1mm Pb+5mm scin.) 12.6 radiation length 0.6cm(T) BBOT readout bar

DISCLAIMER

This report was prepared as an account of work sponsored by an agency of the United States Government. Neither the United States Government nor any agency thereof, nor any of their employees, makes any warranty, express or implied, or assumes any legal liability or responsibility for the accuracy, completeness, or usefulness of any information, apparatus, product, or process disclosed, or represents that its use would not infringe privately owned rights. Reference herein to any specific commercial product, process, or service by trade name, trademark, manufacturer, or otherwise does not necessarily constitute or imply its endorsement, recommendation, or favoring by the United States Government or any agency thereof. The views and opinions of authors expressed herein do not necessarily state or reflect those of the United States Government or any agency thereof.